

**Enzyme Mechanisms**

# The Structural Role of N170 in Substrate-Assisted Deacylation in KPC-2 $\beta$ -Lactamase

Diksha Parwana, Jing Gu, Shuang Chen, Christopher R. Bethel, Emma Marshall, Andrea M. Hujer, Robert A. Bonomo, and Shozeb Haider\*

**Abstract:** The amino acid substitutions in *Klebsiella pneumoniae* carbapenemase 2 (KPC-2) that have arisen in the clinic are observed to lead to the development of resistance to ceftazidime-avibactam, a preferred treatment for KPC bearing Gram-negative bacteria. Specific substitutions in the omega loop (R164-D179) result in changes in the structure and function of the enzyme, leading to alterations in substrate specificity, decreased stability, and more recently observed, increased resistance to ceftazidime/avibactam. Using accelerated rare-event sampling well-tempered metadynamics simulations, we explored in detail the structural role of R164 and D179 variants that are described to confer ceftazidime/avibactam resistance. The buried conformation of D179 substitutions produce a pronounced structural disorder in the omega loop - more than R164 mutants, where the crystallographic omega loop structure remains mostly intact. Our findings also reveal that the conformation of N170 plays an underappreciated role impacting drug binding and restricting deacylation. The results further support the hypothesis that KPC-2 D179 variants employ substrate-assisted catalysis for ceftazidime hydrolysis, involving the ring amine of the aminothiazole group to promote deacylation and catalytic turnover. Moreover, the shift in the WT conformation of N170 contributes to reduced deacylation and an altered spectrum of enzymatic activity.

## Introduction

$\beta$ -lactams, including penicillins, cephalosporins, carbapenems, and monobactams, are the most commonly used antibiotics that irreversibly inhibit enzymes involved in

bacterial cell wall synthesis.<sup>[1]</sup> As a result of persistent exposure to  $\beta$ -lactams and the imposed survival pressure, bacteria continually evolve to evade therapeutic action, predominantly via the production of  $\beta$ -lactamases in Gram-negative bacteria.<sup>[2-5]</sup>  $\beta$ -Lactamases, categorized into classes A, B, C, and D,<sup>[6]</sup> can degrade all classes of  $\beta$ -lactam drugs and thus present a global clinical threat in the form of antimicrobial resistance (AMR).<sup>[7,8]</sup> To combat the ever-increasing AMR, the use of  $\beta$ -lactamase inhibitors- clavulanic acid, tazobactam, and sulbactam that share the  $\beta$ -lactam backbone, were clinically approved in combination with specific  $\beta$ -lactam drugs.<sup>[9]</sup> The emergence of *Klebsiella pneumoniae* carbapenemase (KPC) producing strains, prompted the development of novel  $\beta$ -lactamase inhibitors.<sup>[10]</sup> Efforts to restore activity against these diverse enzymes led to the clinical approval of a non- $\beta$ -lactam (diazabicyclooctane)  $\beta$ -lactamase inhibitor, avibactam.<sup>[11]</sup> Unlike the first three clinical inhibitors that are limited in their activity only to class A  $\beta$ -lactamases, avibactam is a broad-spectrum inhibitor for serine (class A, C, and some class D) enzymes.<sup>[8,12]</sup>

The combination of avibactam with an oxyimino-cephalosporin, ceftazidime, appeared as a salvage therapy for the treatment of carbapenem-resistant Enterobacteriales (CRE) infections primarily caused by KPC-producing bacteria.<sup>[13]</sup> However, a site-directed mutagenesis study revealed ceftazidime-avibactam (CAZ-AVI) resistance in KPC-2 variants with substitutions at R164 and D179 positions of the omega loop.<sup>[14,15]</sup> Similar resistance was reported for an in vitro study for KPC-3 expressing Enterobacteriaceae, primarily due to a D179Y substitution.<sup>[16]</sup> Shortly after, CAZ-AVI resistance was demonstrated in clinical isolates being treated

[\*] D. Parwana, J. Gu, S. Chen, S. Haider  
 UCL School of Pharmacy, London, UK

C. R. Bethel, E. Marshall, A. M. Hujer, R. A. Bonomo  
 Research Service, Louis Stokes Cleveland Department of Veterans  
 Affairs Medical Center, Cleveland, OH, USA

A. M. Hujer, R. A. Bonomo  
 Department of Medicine, Case Western Reserve University School  
 of Medicine, Cleveland, OH, USA

R. A. Bonomo  
 Clinician Scientist Investigator, Louis Stokes Cleveland Department  
 of Veterans Affairs Medical Center, Cleveland, OH, USA  
 and

Department of Molecular Biology and Microbiology, Pharmacology,  
 Biochemistry, and Proteomics and Bioinformatics, Case Western  
 Reserve University School of Medicine, Cleveland, OH, USA  
 and

CWRU-Cleveland VAMC Center for Antimicrobial Resistance and  
 Epidemiology (Case VA CARES) Cleveland, OH, USA

S. Haider  
 UCL Centre for Advanced Research Computing,  
 London, UK  
 E-mail: Shozeb.haider@ucl.ac.uk

© 2024 The Authors. Angewandte Chemie International Edition published by Wiley-VCH GmbH. This is an open access article under the terms of the Creative Commons Attribution Non-Commercial NoDerivs License, which permits use and distribution in any medium, provided the original work is properly cited, the use is non-commercial and no modifications or adaptations are made.

for KPC-expressing CRE infections with this  $\beta$ -lactam-inhibitor combination.<sup>[17]</sup> A series of studies using site-saturation and site-directed mutagenesis uncovered the complex array of substitutions conferring ceftazidime/avibactam resistance.<sup>[18–20]</sup>

The omega loop (residues R164–D179 in KPC-2) (Figure 1) plays a vital role in the  $\beta$ -lactamase enzymatic mechanism. Following the nucleophilic attack by S70, the acyl-enzyme complex is deacylated by a conserved water molecule that is strategically held in position by omega loop residues E166 and N170. E166 acts as the general base that activates the water molecule for the subsequent attack on the covalent complex.<sup>[21,22]</sup> However, in light of the development of ceftazidime-avibactam resistance in clinical isolates and the impacted kinetics of ceftazidime deacylation reported by recent experiments, we aimed to uncover the underlying mechanisms of altered enzymatic activity for KPC-2 mutants. This study investigates the perturbed structural dynamics involving the omega loop region as a result of six significant KPC-2 omega loop substitutions—R164S,<sup>[23]</sup> R164H,<sup>[24–26]</sup> D179N,<sup>[14,27–30]</sup> D179Y,<sup>[18,19,23,28,29,31–35]</sup> D179A,<sup>[36–38]</sup> and D179Q<sup>[27]</sup> that have shown to confer resistance against CAZ-AVI combination. Residues R164 and D179 confer stability to the omega loop by interacting via a salt bridge. Thus, a substitution at either position might cause pronounced structural changes to the middle of the loop, harboring critical catalytic residues.

Using well-tempered metadynamics (wt-MetaD), we accelerated rare-event sampling and uncovered important conformational changes upon R164 or D179 substitution.<sup>[39]</sup> Due to the buried conformation of D179, variants at this position produce a more pronounced structural disorder in

the omega loop compared to R164 mutants, where the crystallographic structure remains mostly intact.<sup>[30,40]</sup> The findings suggest that the conformation of the omega loop with N170 oriented “away” is favored for KPC-2 omega loop mutants, impacting drug binding and restricting deacylation. This work further strengthens the notion that KPC-2 D179 variants employ substrate-assisted catalysis for ceftazidime, involving the ring amine of the aminothiazole group to promote deacylation and catalytic turnover. Our study attempts to answer the perplexing questions pertaining to the enhanced resistance of KPC-2 mutants to ceftazidime/avibactam intervention as a result of omega loop substitutions. With the emerging resistant strains imposing a major clinical challenge, our results hold significant importance for future drug design.

## Results and Discussion

### D179 variants exhibit altered conformational dynamics

Well-tempered Metadynamics (wt-MetaD) allows us to investigate the most favored conformations of KPC-2 variants, typically separated by large energy barriers and thus challenging to conventional MD simulations.<sup>[39,41,42]</sup> By forcing the system to escape local minima, wt-MetaD simulations explore the least populated regions of the system within the collective variable (CV) space. The conformations corresponding to the reconstructed free energy minima may shed light on the key regulatory changes and altered enzymatic mechanisms. To understand how mutations alter the dynamics of our system, we character-

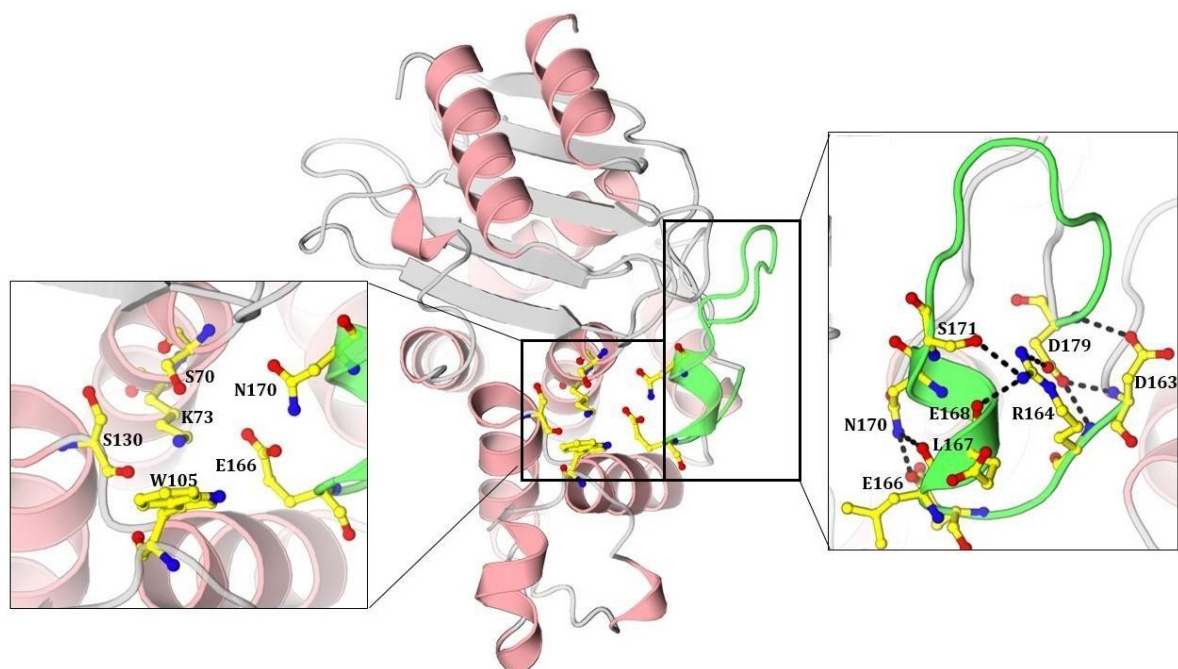


**Figure 1.** Structure of KPC-2  $\beta$ -lactamase (PDB id: 3DW0) highlighting important active site residues (left) and omega loop interactions (right). The omega loop is colored green.

ized the free energy landscape as a function of backbone dihedral angles ( $\phi$  and  $\psi$ ) as they represent the true slow dynamics and could describe global behavior.<sup>[43,44]</sup> Hence, our wt-MetaD simulations were biased to two CVs— the backbone  $\phi$  and  $\psi$  dihedral angles of the alerted residue under study, that is, residue 164 for R164 mutants and residue 179 for D179 mutants. Additionally, two different free energy plots for KPC-2 WT were computed using CVs corresponding to residues R164 and D179.

The free energy surface (FES) for WT as a function of D179-related CVs exhibits one local minimum indicating similar interactions as seen for the native crystal structure (PDB id- 3DW0) (Figure S1). Upon back mapping, we observed that the crystal structure lies in the largest free energy minima; thus, it represents the most stable omega loop conformation presenting R164-D179, R164-S171, D179-D163, and E166-N170 interactions.

The FES plot for D179N involves two minima as shown in Figure 2. The extracted conformations unravel the disrupted H-bonding network due to the loss of the R164-

D179 salt bridge at the neck of the omega loop (Figure S1). In basin B, R164 adopts a solvent-exposed conformation, unable to maintain its native interactions by virtue of D179 substitution and a consequent dynamic loop. Basin A (7 kcal/mol lower in energy than basin B), on the other hand, depicts R164 intact due to the shift in D176 that leads to the formation of the R164-D176 salt bridge. Interestingly, both the conformations sampled by wt-MetaD capture N170 displaced from its crystallographic pose, unable to position the water molecule for effective deacylation of the acyl-enzyme complex. In basin A, the displaced N170 interacts with the backbone of L167, while in the other basin, the shift in the N170 side chain forms new interactions with the backbone of T237 and G238 (consensus numbering). An increased distance from E166 and the formation of new interactions abate the basic character of N170 that is required to activate the deacylating water molecule. Biochemical analysis reporting a decreased rate of deacylation for the hydrolysis of imipenem as well as ceftazidime in D179N strains could be attributed to N170 displacement.<sup>[27]</sup>

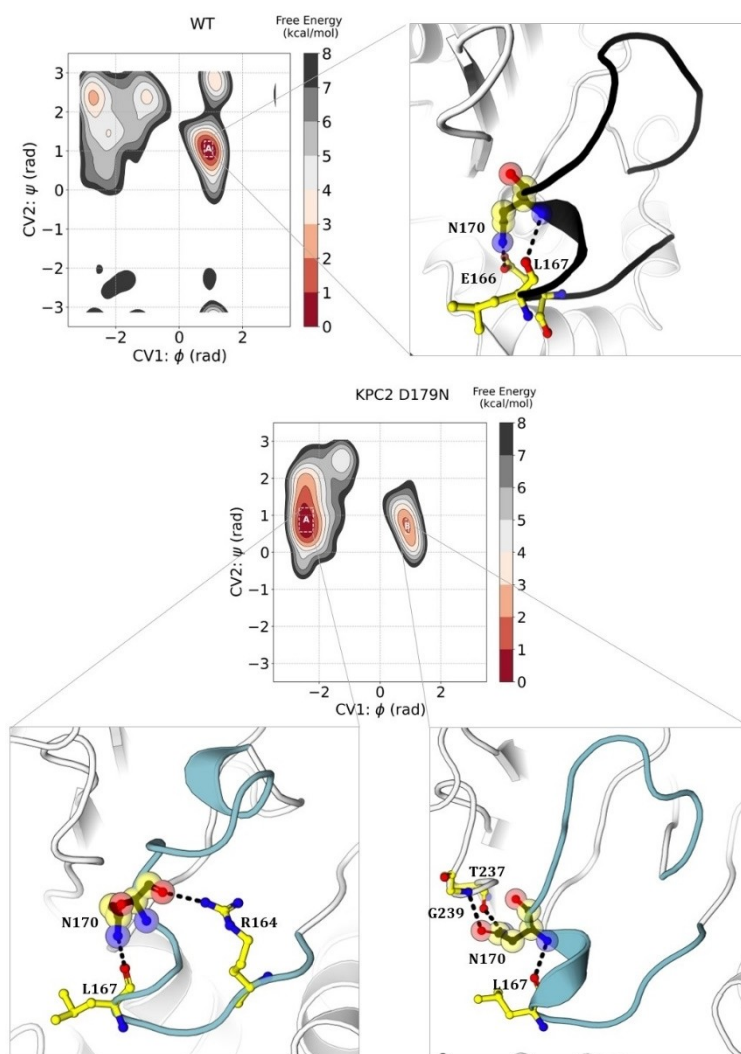


**Figure 2.** Free energy plots for KPC-2 WT (top) and D179N (bottom) as a function of  $\phi$  (CV1) and  $\psi$  (CV2) dihedral angles of residue 179. The interactions of N170 present in the omega loop (WT—black; D179N—cyan) extracted from their corresponding free energy minima are illustrated.

The shift in N170 leading to slower hydrolysis further explains the proposition of preferential trapping of  $\beta$ -lactams when compared to avibactam in the expanded active site of D179N mutants.<sup>[27]</sup> The deacylation mechanism of avibactam in D179N likely involves S130 and K73; thus, its enzymatic kinetics remain unaffected with the shift in N170.<sup>[45]</sup> Due to the reduced deacylation rates for  $\beta$ -lactams in the D179N mutant, we suggest the shift in the WT conformation of N170 as the underlying cause for impacted deacylation and altered spectrum of enzymatic activity. Moreover, N170A substitution in KPC-2 exhibited a >3000-fold reduction in the deacylation rate for imipenem hydrolysis in a site-directed mutagenesis study.<sup>[46]</sup> Thus, the crucial involvement of N170 in KPC-2  $\beta$ -lactamase activity is further supported by the decreased hydrolytic activity upon N170 substitution.

In the D179Y KPC-2 variant, R164 forms a double salt bridge with D176 (basin B and C) or with D163 (basin A) (Figure S2). Also, in basin A (1 kcal/mol and 1.8 kcal/mol

lower in energy than basin B and C respectively), R164-S171 sidechain-sidechain interaction is observed, similar to WT KPC-2. Substitution of the negatively charged carboxyl group with a phenol moiety results in a highly flexible structure that leads to the disruption of the H-bond network formed by the buried conformation of D179 in WT. Contrastingly, D179Y adopts an exposed conformation, unable to form interactions within the loop (Figure 3). The lost structural integrity of the omega loop limits the binding of diverse classes of  $\beta$ -lactams in a distorted active site resulting in lower MICs for penicillins (ampicillin, piperacillin), carbapenems (imipenem, meropenem), cephalosporins (cefepime, ceftriaxone, cefotaxime) as well as monobactams (aztreonam).<sup>[19,20]</sup> The deformed omega loop fails to define the binding pocket anymore and might not be able to sustain the structural changes associated with the binding of a  $\beta$ -lactam in the pocket, thus impeding catalysis. Moreover, the disruption of stabilizing omega loop inter-

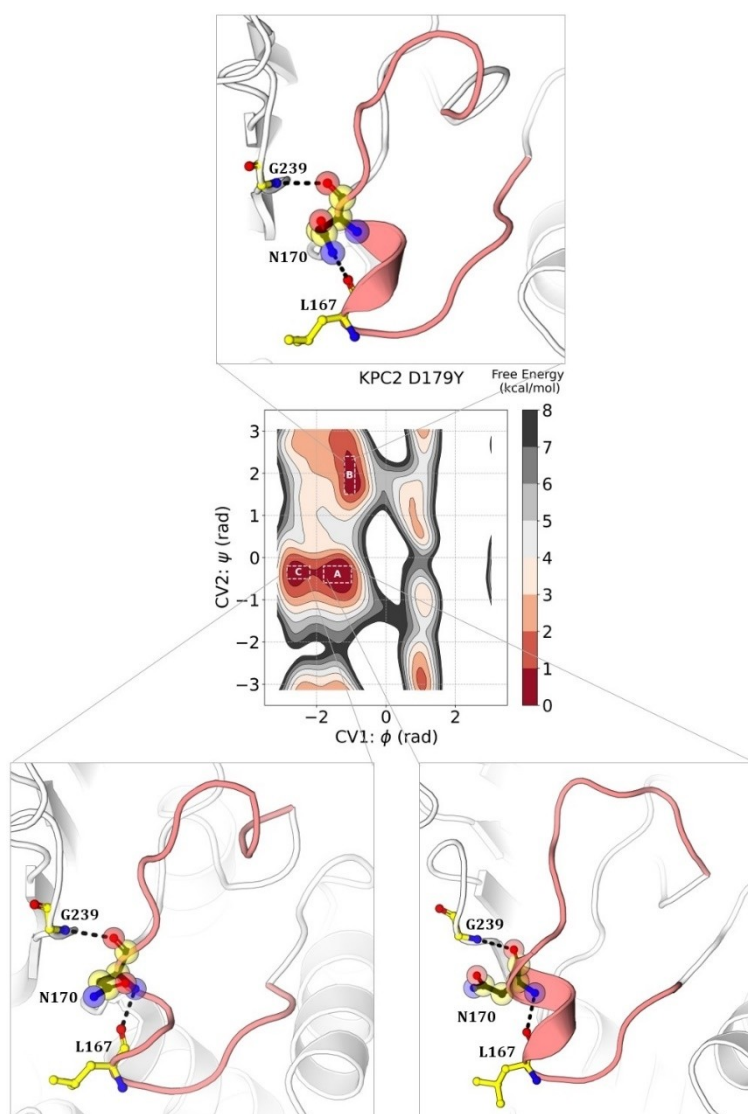


**Figure 3.** Free energy plot for KPC-2 D179Y as a function of  $\phi$  (CV1) and  $\psi$  (CV2) dihedral angles of residue 179. The interactions of N170 present in the omega loop (salmon) extracted from their corresponding free energy minima are illustrated.

actions is unable to constrain N170 in its native conformation involved in the deacylation reaction. Its side chain flips away from the active site and interacts with the L167 main chain (basin B) or remains disengaged (basin A and basin C). The distance of basic carbonyl oxygen of the N170 side chain from the water molecule increases to more than 5 Å in all three observed basins. As a result, slower deacylation might also contribute to the decreased resistance of KPC-2 D179Y mutants to various  $\beta$ -lactams.

In the D179A mutant, due to the loss of the R164-D179 salt bridge, the side chain of R178 shifts closer to D163, resulting in a salt bridge as revealed by the most stable conformations observed in basin A as well as basin C (2.8 kcal/mol higher in energy than basin A) (Figure S3). In another free energy minima, basin D (3 kcal/mol higher than basin A), R164 shows a new interaction in the form of an ionic bond with the displaced D176 and maintains its native

interaction with the sidechain of S171. The helix encompassing E166 and N170 unfolds, and a shift in the side chain of N170 with respect to the WT conformation is observed in all four free energy minima. The substitution of acidic aspartic acid with hydrophobic alanine causes the side chain of N170 to orient away from the active site towards the altered residue A179 (Figure 4). In the most stable conformation (basin A), the side chain of N170 forms an H-bond with the backbone of A179 and L68. A similar conformation of N170 is observed in basin B as its side chain rotates away from the active site, interacting with the backbone of T180 towards the end of the omega loop. This shift in the N170 side chain, while providing access to an expanded active site, might impede effective deacylation of other  $\beta$ -lactams but not ceftazidime.

The substitution of aspartic acid with glutamine in KPC-2 D179Q results in the opening of the omega loop due to

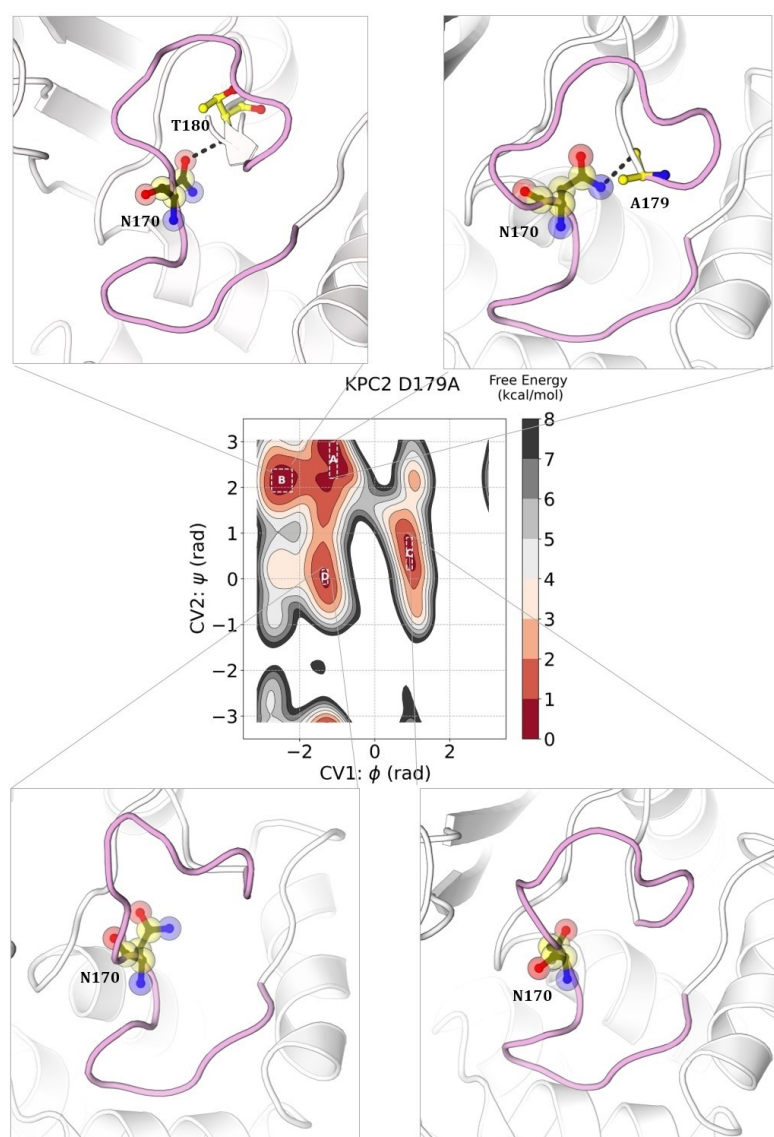


**Figure 4.** Free energy plot for KPC-2 D179A as a function of  $\phi$  (CV1) and  $\psi$  (CV2) dihedral angles of residue 179. The orientation and interactions of N170 present in the omega loop (pink) extracted from their corresponding free energy minima are illustrated.

the absence of integral bonds at the neck of the structure (Figure 5). Consequently, R164 fails to stay intact with respect to its WT orientation and either interacts with E168 (basin A and B) or S171 (basin C). The particularly dynamic motions of D176 and Q179 arising due to changes in the conformational equilibrium engender a disintegrated overlying region of the omega loop (Figure S4). Enhanced mobility as a result of D179Q mutation in the omega loop is transmitted to the active site residue N170, resulting in the disruption of E166-N170 interaction. Unlike other clinically observed D179 substitutions included in this study, D179Q mutation has not been reported in clinical isolates. Its altered spectrum of activity has been studied using saturation mutagenesis studies *in vitro*.<sup>[27]</sup>

For D179 variants (D179N, D179Y, D179A, and D179Q), conformations extracted from the free energy minima outline the enhanced flexibility of the omega loop due to the disruption of the R164-D179 salt bridge. Concomitant with the unstable omega loop is the displacement of the N170 side chain away from the active site,

unable to interact with E166 and prime the water molecule for deacylation. While the profound fluctuation of N170 is consistent for each energetically stable conformation for all D179 mutants, the omega loop mutation doesn't seem to distort E166, which maintains its WT-like conformation facing the active site throughout the sampling time. This leads us to reason the shift in N170 as the underlying cause for lowered deacylation rate of D179 mutants for ceftazidime as well as other  $\beta$ -lactams. As for binding kinetics, the compromised structural integrity of the omega loop renders the active site inefficient to accommodate typically small  $\beta$ -lactam drugs causing D179 variants to become susceptible to several classes of  $\beta$ -lactams. However, increased omega loop flexibility with N170 oriented away is likely to aid in the binding of bulky  $\beta$ -lactam, like ceftazidime and thereby giving rise to enhanced resistance of KPC-2 variants to the ceftazidime-avibactam combination. Results of previous studies on GES type class A  $\beta$ -lactamases reveal the variation in the kinetics of hydrolysis of a non-bulky carbapenem, imipenem, with other comparatively bulkier  $\beta$ -

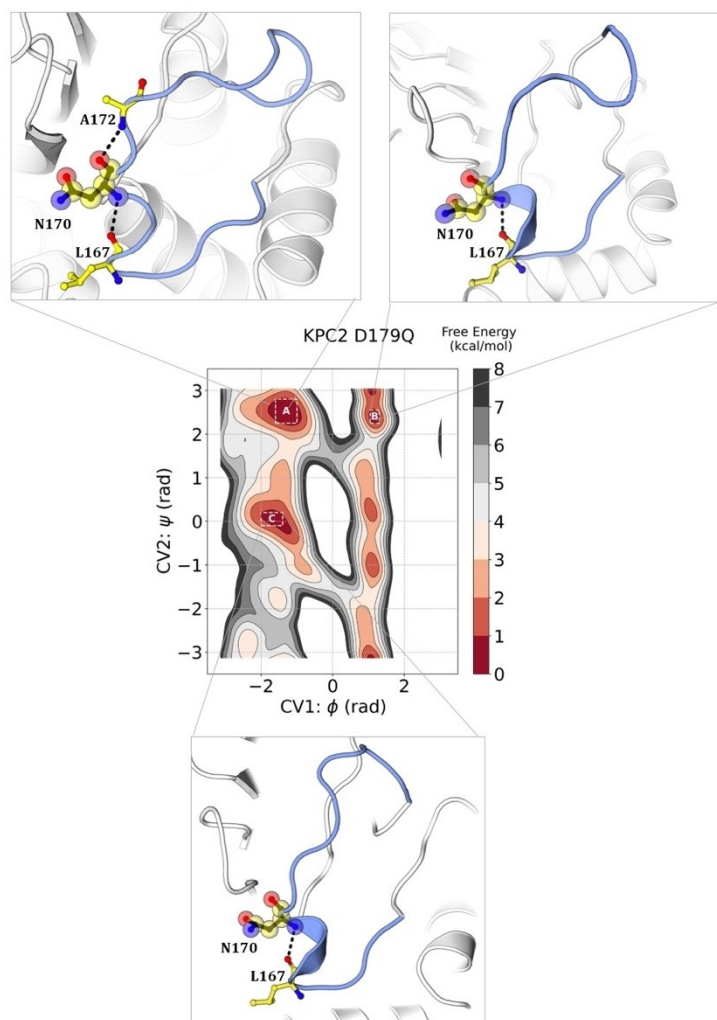


**Figure 5.** Free energy plot for KPC-2 D179Q as a function of  $\phi$  (CV1) and  $\psi$  (CV2) dihedral angles of residue 179. The interactions of N170 present in the omega loop (blue) extracted from their corresponding free energy minima are illustrated.

lactams.<sup>[47]</sup> Our findings reveal the basis for altered substrate specificity for the active site of KPC-2 mutants in the context of rising CAZ-AVI resistance.

### Displaced N170 impacts $\beta$ -lactamase activity

In the most favored conformations of D179 mutants, a significant alteration is observed in the direction of N170 due to the absence of the R164-D179 salt bridge. KPC-2 D179 mutants also present a modest shift in the side chain of S70 by 1.5 Å, whereas other catalytic residues i.e., K73, S130, and E166, maintain their overall WT-like conformations. While D179 mutants develop increased resistance to ceftazidime, their activity against other  $\beta$ -lactam drugs diminishes. Kinetic studies report lower MICs and decreased turnover ( $k_{\text{cat}}$ ) in the hydrolysis of several penicillins, carbapenems, cephalosporins, as well as monobactams, especially for the D179Y mutant.<sup>[18,19,24,32,33,48]</sup> This elevated susceptibility of KPC-2 D179 strains to various  $\beta$ -lactams is attributed to the highly disordered omega loop that limits the effective hydrolysis of  $\beta$ -lactams. The disorientation of N170 results in an expanded binding pocket (Figure S5) and impedes the deacylation of the acyl-enzyme complex. The displaced S70 side chain might additionally restrict the acylation of the substrate.<sup>[27]</sup> Paradoxically, the repositioning of the N170 side chain eases the accommodation of the bulky  $\beta$ -lactam, ceftazidime, due to the concomitant expansion of the binding pocket. Docking of ceftazidime in the active site of KPC-2 variants indicates the orientation of the aminothiazole ring of C7 substituent of ceftazidime towards WT conformation of N170, thus highlighting the potential bypass of steric clashes upon N170 displacement. As a result of N170 being directed away from the active site, ceftazidime is able to bury more profoundly in the cavity, as exhibited by the docked complexes of acylated ceftazidime in the binding pocket of D179 variants (Figure S6–S10). For orderly ceftazidime binding, omega loop restructuring that drives a disparate conformation of N170 appears necessary. This is also indicated by the MD simulations of ceftazidime acyl-enzyme complex with WT KPC-2.<sup>[20]</sup> The resulting enhanced ceftazidime binding for KPC-2 variants is in agreement with kinetic studies that report reduced  $K_{\text{m}}$  values and propose that the elevated kinetics of ceftazidime binding is the focal cause for CAZ-AVI resistance.<sup>[19,30,49]</sup> While the shift in N170 causes active site expansion and promotes increased binding affinity for the bulky cephalosporin, the deacylation mechanism, where N170 is involved in priming the water molecule, is compromised. Our findings are in accordance with kinetic and mass spectrometry assays that report slower ceftazidime hydrolysis/turnover by D179 variants compared to the WT  $\beta$ -lactamase. The catalytic turnover ( $k_{\text{cat}}$ ), as well as hydrolytic efficiency ( $k_{\text{cat}}/K_{\text{m}}$ ), decreases for ceftazidime, due to the reduced rate of deacylation. The “trapping” of  $\beta$ -lactams, as suggested by various kinetic studies, could be explained by the lowered rate of deacylation and slower hydrolysis by virtue of N170 displacement.<sup>[19,27,29,37]</sup> However, the variants are still able to hydrolyze ceftazidime leading to overall increased MIC and

drug resistance. This is unique to ceftazidime due to its bulky component, the aminothiazole ring on the C7 substituent, that is able to position in the pocket when N170 displaces away.<sup>[29]</sup> In a broad sense, we propose that the altered susceptibility of KPC-2 variants to different  $\beta$ -lactam drugs is due to the active site expansion and N170 displacement. The loss of the stabilizing omega loop interactions results in a highly flexible structure unable to constrain N170 in its deacylation-competent orientation.

### D179 variants (D179N and D179Y) exhibit substrate-assisted catalysis for ceftazidime

We have demonstrated that the shift in N170 accounts for the high binding affinity for ceftazidime. However, the increased resistance to ceftazidime-avibactam cannot be solely attributed to improved drug entrapment. Questions arise about how complete hydrolysis of ceftazidime is achieved if the displaced N170 conformation impedes deacylation. Does N170 return to its original state after drug binding to deacylate the acyl-enzyme complex or is there an alternative mechanism that facilitates effective deacylation to regenerate the active site? We postulate that when N170 is oriented away from the active site, the ring amine or the primary amine of the aminothiazole group in ceftazidime is ideally positioned to activate the water molecule, initiating an attack on the covalent complex. Successful deacylation step in  $\beta$ -lactam hydrolysis requires a water molecule near the acylated intermediate's carbonyl group and a nearby general base for water activation. In the absence of a base proximal to the active site in class-C  $\beta$ -lactamases, it was proposed that the  $\beta$ -lactam nitrogen, which is a secondary amine nitrogen post acylation and  $\beta$ -lactam ring opening, can activate the water molecule.<sup>[50]</sup> We propose a similar activation of the conserved water molecule is initiated via the aminothiazole group of ceftazidime in KPC-2 variants. Superimposition of the docked ceftazidime in the D179N active site with the WT revealed the distance between the water molecule and that of primary amine nitrogen and ring amine nitrogen to be 3.2 and 3.6 Å, respectively (Figure S9). Similarly, for D179Y, the respective distances are 3.8 and 4.1 Å (Figure S10). We posit that the aminothiazole group enhances the possibility of an attack on the water molecule by two nitrogen atoms within its vicinity. This way, the substrate itself promotes the approach of the deacylating water molecule to the acyl-enzyme complex.

### D179 variants show increased susceptibility to moxalactam

Moxalactam (MOX) is categorized within the expanded spectrum cephalosporins, yet it differs by having an oxygen atom substitute the sulfur atom of the cephem nucleus (Figure S6). This synthetic oxacephem antibiotic exhibits potent antibacterial efficacy against ESBL-producing bacterial strains.<sup>[51]</sup> While the kinetic studies suggesting its activity against KPC-producing strains are limited, *E. coli* harboring KPC-6 (V240G) reported elevated resistance to MOX with

increased MIC.<sup>[52]</sup> Our investigation focused on understanding how mutations at position 179 in the omega loop in KPC affect the hydrolyzing profile of MOX. The emerging bacterial strains harboring KPC-2 substitutions demonstrated varying hydrolyzing activity/susceptibility for the two drugs (Table 1). We propose that the structural alterations in the active site resulting from omega loop mutations render the enzyme incapable of carrying out substrate-assisted deacylation with MOX. The hindered deacylation mechanism allows for complete hydrolysis governed by distinctive structural characteristics of the substrate itself. In case of ceftazidime, although the deacylation mechanism is compromised due to N170 displacement, the positioning of the aminothiazole ring, a crucial structural component with two potential basic nitrogen atoms facilitates the deacylation of the carbonyl complex, resulting in complete albeit slower  $\beta$ -lactam hydrolysis. Conversely, KPC-2 mutants with D179 substitutions are likely to become susceptible to drugs like MOX, where the antibiotic structure lacks the aminothiazole ring necessary for the deacylation process. The absence of an aminothiazole ring or a similar structural feature completely eliminates the possibility of substrate-assisted catalysis, as observed for MOX. Thus, KPC-2 mutants lose their ability to hydrolyze MOX (confer resistance) as well as other  $\beta$ -lactams, and the antibacterial activity of this cephalosporin is restored. Mass spectrometry of MOX with D179Y showed a prolonged acyl-enzyme complex (Figure 6). There is fragmentation of MOX and only the 405 Da adduct is present. The proposed reaction mechanism for this fragmentation is provided (Figure S11).

### R164 mutants (R164S and R164H) also present a shift in N170 leading to CAZ-AVI resistance

To investigate the modified conformational landscape of R164S and R164H, we used the backbone dihedral angles of residue R164 to characterize the free energy surface. The free energy plots resulted in one basin for both R164S and R164H mutants. (Figure S12) The extracted conformations highlight the overall conserved omega loop structure, unlike D179 mutants, where the loop becomes disordered as a consequence of R164-D179 salt bridge disruption. Due to the substitution of arginine with serine and histidine in R164S and R164H KPC-2, respectively, the native interactions R164-D179, R164-S171, and R164-E168 are lost in the variant enzymes. However, as a result of the solvent-exposed conformation of R164, the substitution at this position doesn't drastically perturb the orientation of other residues within or outside the loop. Our analysis shows that the fluctuation in the loop of R164 mutants is not as dynamic as in D179 mutants, but the E166-N170 interaction is still lost. Similar to D179 KPC variants, R164S and R164H KPC-2 also present a shift in the side chain of N170, where it moves out facing away from the active site. We propose that the altered enzymatic activity of KPC-2 bearing substitutions at 164 and 179 positions of the omega loop is due to the modified conformation of N170. With the side chain of N170 moved out, the mutant enzymes are primed to accommodate the bulky aminothiazole group of ceftazidime, resulting in enhanced kinetics of ceftazidime binding. This has also been suggested earlier by circular dichroism experiments for KPC-2 R164S mutant.<sup>[24]</sup> The structural perturba-

**Table 1:** MICs of  $\beta$ -lactam and  $\beta$ -lactam- $\beta$ -lactamase inhibitor combinations against KPC-2 D179 and R164 variants.

Strain = <i>E. coli</i> DH10B Vector = pBR322	MICs ( $\mu\text{g/ml}$ )					
	CAZ	AZT	MOX	CAZ/AVI	AZT/AVI	MEM
Empty vector control	0.5	0.5	0.25	$\leq 0.25$	0.125	$\leq 0.06$
KPC-2 (WT)	64	> 256	16	$\leq 0.25$	0.125	8
KPC-2 (164D/179R)	256	4	2	8	0.25	$\leq 0.06$
KPC-2 164A	256	128	4	8	0.25	0.125
KPC-2 164H	256	> 256	16	4	0.25	1
KPC-2 164P	128	16	8	16	0.25	$\leq 0.06$
KPC-2 164S	256	128	8	4	0.25	0.5
KPC-2 179A	512	8	2	16	0.25	$\leq 0.06$
KPC-2 179R	16	1	2	8	0.25	$\leq 0.06$
KPC-2 179N	512	> 256	8	16	0.5	2
KPC-2 179Q	128	4	4	8	0.5	$\leq 0.06$
KPC-2 179G	512	32	4	16	0.5	$\leq 0.06$
KPC-2 179H	256	32	2	32	0.5	$\leq 0.06$
KPC-2 179I	32	4	0.5	$\leq 0.25$	0.25	$\leq 0.06$
KPC-2 179L	512	4	4	16	0.25	$\leq 0.06$
KPC-2 179K	64	1	2	8	0.25	$\leq 0.06$
KPC-2 179M	512	64	4	32	0.5	$\leq 0.06$
KPC-2 179F	256	16	4	32	0.5	$\leq 0.06$
KPC-2 179P	256	4	4	32	0.5	$\leq 0.06$
KPC-2 179S	128	32	4	16	0.25	$\leq 0.06$
KPC-2 179T	256	8	2	16	0.25	$\leq 0.06$
KPC-2 179W	> 512	16	4	32	0.25	$\leq 0.06$
KPC-2 179Y	512	16	4	32	0.5	$\leq 0.06$
KPC-2 179V	512	8	4	32	0.5	$\leq 0.06$

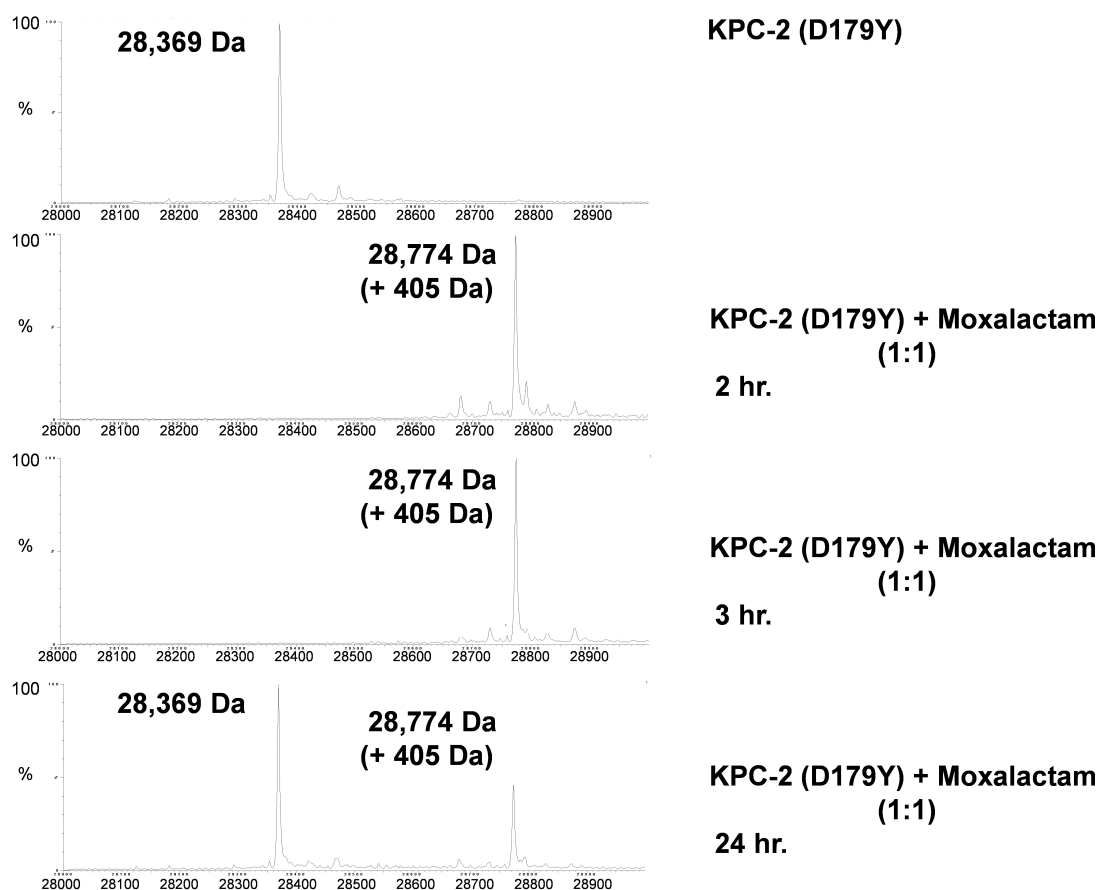


**Figure 6.** Timed mass spectrometry. The KPC-2 D179Y variant forms a prolonged (24 h) acyl complex with moxalactam.

tion of N170 around the active site translates to the ceftazidime avibactam resistance phenotype. The lack of stabilizing salt bridge interaction at the neck of the omega loop drives N170 displacement and a consequent expanded binding pocket. However, the flexible omega loop renders the enzyme incapable of sustaining structural deformations required for the binding of several other drugs like ampicillin, cephalothin, cefotaxime, cefepime, aztreonam, and imipenem.<sup>[24]</sup>

The deacylation mechanism is also impaired, resulting in reduced MICs to these drugs. For KPC-2 omega loop mutants, we observe a different conformation of N170 in the apo-enzyme as a result of omega loop mutation, whereas for SHV-type  $\beta$ -lactamase, this structural disorder is only noticed upon binding of the ligand.<sup>[40]</sup> Since there is a ligand-induced disorder, ceftazidime binding faces initial resistance due to potential steric clashes between the aminothiazole group and N170 facing the active site. Thus,  $K_m$  for ceftazidime slightly increases for SHV-1  $\beta$ -lactamase, as opposed to KPC-2, where  $K_m$  decreases, and enhanced binding affinity for ceftazidime is identified as the resistant determinant.<sup>[40]</sup>

## Conclusion

In summary, the application of wt-MetaD simulations, microbiological, biochemical and crystallographic analysis of these omega loop variants enhance our understanding of this extremely problematic phenotype resulting in ceftazidime avibactam resistance. In terms of future drug development, the underappreciated role of the aminothiazole group in substrate-assisted catalysis is a starting point for developing novel  $\beta$ -lactams. The unexpected increase in susceptibility to the representative oxacephem suggests a path forward in the design of novel cepheems. Further studies exploring the interactions of carbapenems or carbapenem mimics in these variants will also further illuminate their potential role as carbapenemase inhibitors.

## Supporting Information

Supporting Information contains Figures S1–S23, Table S1.

## Author Contribution

Simulations—Diksha Parwana; Analysis—Diksha Parwana, Jing Gu, Shuang Chen; Mass Spectrophotometry—Chris

Bethel, Emma Marshall, Andrea Hujer; MIC experiments—Chris R. Bethel, Emma Marshall, Andrea M. Hujer; Supervision—Robert A. Bonomo and Shozeb Haider. All authors contributed in the preparation of the manuscript.

### Acknowledgements

This work was supported in part by funds and/or facilities provided by the Cleveland Department of Veterans Affairs, Award Number 1101BX001974 (R.A.B.), from the Biomedical Laboratory Research & Development Service of the VA Office of Research and Development, and the Geriatric Research Education and Clinical Center VISN 10. The content is solely the authors' responsibility and does not necessarily represent the official views of the NIH or the Department of Veterans Affairs. RAB is also supported by Merck, VenatoRx, Entasis, Shionogi, Wockhardt for research support only. All other authors declare no conflict of interest.

### Conflict of Interest

RAB is also supported by Merck, VenatoRx, Entasis, Shionogi, Wockhardt for research support only.

### Data Availability Statement

All simulation data can be downloaded from <https://doi.org/10.5281/zenodo.8433386>.

**Keywords:**  $\beta$ -lactam antibiotics ·  $\beta$ -lactamase · metadynamics · substrate-assisted catalysis · enhanced sampling

- [1] K. Bush, P. A. Bradford, *Cold Spring Harbor Perspect. Med.* **2016**, *6*, a025247.
- [2] F. C. Tenover, *The American Journal of Medicine* **2006**, *119*, S3–S10.
- [3] K. Bush, *Antimicrob. Agents Chemother.* **2018**, *62*, e01076–18.
- [4] C. A. Arias, B. E. Murray, *N. Engl. J. Med.* **2009**, *360*, 439–443.
- [5] J. F. Fisher, J. R. Knowles, in *Annual Reports in Medicinal Chemistry*, Elsevier, **1978**, pp. 239–248.
- [6] K. Bush, G. A. Jacoby, *Antimicrob. Agents Chemother.* **2010**, *54*, 969–976.
- [7] R. A. Bonomo, *Cold Spring Harbor Perspect. Med.* **2017**, *7*, a025239.
- [8] C. L. Tooke, P. Hinchliffe, E. C. Bragginton, C. K. Colenso, V. H. A. Hirvonen, Y. Takebayashi, J. Spencer, *J. Mol. Biol.* **2019**, *431*, 3472–3500.
- [9] S. M. Drawz, R. A. Bonomo, *Clin. Microbiol. Rev.* **2010**, *23*, 160–201.
- [10] L. Chen, A. Paterson, *IDR* **2012**, 133.
- [11] D. E. Ehmann, H. Jahić, P. L. Ross, R.-F. Gu, J. Hu, G. Kern, G. K. Walkup, S. L. Fisher, *Proc. Natl. Acad. Sci. USA* **2012**, *109*, 11663–11668.
- [12] C. Fröhlich, J. Z. Chen, S. Gholipour, A. N. Erdogan, N. Tokuriki, *Protein Eng. Des. Sel.* **2021**, *34*, gzab013.
- [13] G. G. Zhanel, C. D. Lawson, H. Adam, F. Schweizer, S. Zelenitsky, P. R. S. Lagacé-Wiens, A. Denisuik, E. Rubinstein, A. S. Gin, D. J. Hoban, J. P. Lynch, J. A. Karlowsky, *Drugs* **2013**, *73*, 159–177.
- [14] M. L. Winkler, K. M. Papp-Wallace, R. A. Bonomo, *J. Antimicrob. Chemother.* **2015**, *70*, 2279–2286.
- [15] B. Spellberg, R. A. Bonomo, *Clin. Infect. Dis.* **2016**, *63*, 1619–1621.
- [16] D. M. Livermore, M. Warner, D. Jamroz, S. Mushtaq, W. W. Nichols, N. Mustafa, N. Woodford, *Antimicrob. Agents Chemother.* **2015**, *59*, 5324–5330.
- [17] R. K. Shields, B. A. Potoski, G. Haidar, B. Hao, Y. Doi, L. Chen, E. G. Press, B. N. Kreiswirth, C. J. Clancy, M. H. Nguyen, *Clin. Infect. Dis.* **2016**, *63*, 1615–1618.
- [18] R. K. Shields, L. Chen, S. Cheng, K. D. Chavda, E. G. Press, A. Snyder, R. Pandey, Y. Doi, B. N. Kreiswirth, M. H. Nguyen, C. J. Clancy, *Antimicrob. Agents Chemother.* **2017**, *61*, e02097–16.
- [19] F. Compain, M. Arthur, *Antimicrob. Agents Chemother.* **2017**, *61*, e00451–17.
- [20] C. L. Tooke, P. Hinchliffe, R. A. Bonomo, C. J. Schofield, A. J. Mulholland, J. Spencer, *J. Biol. Chem.* **2021**, *296*, 100126.
- [21] J. F. Fisher, S. O. Meroueh, S. Mobashery, *Chem. Rev.* **2005**, *105*, 395–424.
- [22] J. C. Hermann, L. Ridder, H.-D. Höltje, A. J. Mulholland, *Org. Biomol. Chem.* **2006**, *4*, 206–210.
- [23] M. Castanheira, S. J. R. Arends, A. P. Davis, L. N. Woosley, A. A. Bhalodi, S. H. MacVane, *mSphere* **2018**, *3*, e00408–18.
- [24] P. S. Levitt, K. M. Papp-Wallace, M. A. Taracila, A. M. Hujer, M. L. Winkler, K. M. Smith, Y. Xu, M. E. Harris, R. A. Bonomo, *J. Biol. Chem.* **2012**, *287*, 31783–31793.
- [25] J. Findlay, L. Poirel, M. Juhas, P. Nordmann, *Antimicrob. Agents Chemother.* **2021**, *65*, e00890–21.
- [26] S. Göttig, D. Frank, E. Mungo, A. Nolte, M. Hogardt, S. Besier, T. A. Wichelhaus, *J. Antimicrob. Chemother.* **2019**, *74*, 3211–3216.
- [27] M. D. Barnes, M. L. Winkler, M. A. Taracila, M. G. Page, E. Desarbre, B. N. Kreiswirth, R. K. Shields, M.-H. Nguyen, C. Clancy, B. Spellberg, K. M. Papp-Wallace, R. A. Bonomo, *mBio* **2017**, *8*, e00528–17.
- [28] L. Sun, W. Chen, H. Li, L. Li, X. Zou, J. Zhao, B. Lu, B. Li, C. Wang, H. Li, Y. Liu, B. Cao, *J. Antimicrob. Chemother.* **2020**, *75*, 3072–3074.
- [29] T. A. Alsenani, S. L. Viviani, V. Kumar, M. A. Taracila, C. R. Bethel, M. D. Barnes, K. M. Papp-Wallace, R. K. Shields, M. H. Nguyen, C. J. Clancy, R. A. Bonomo, F. Van Den Akker, *Antimicrob. Agents Chemother.* **2022**, *66*, e02414–21.
- [30] S. Marshall, A. M. Hujer, L. J. Rojas, K. M. Papp-Wallace, R. M. Humphries, B. Spellberg, K. M. Hujer, E. K. Marshall, S. D. Rudin, F. Perez, B. M. Wilson, R. B. Wasserman, L. Chikowski, D. L. Paterson, A. J. Vila, D. Van Duin, B. N. Kreiswirth, H. F. Chambers, V. G. Fowler, M. R. Jacobs, M. E. Pulse, W. J. Weiss, R. A. Bonomo, *Antimicrob. Agents Chemother.* **2017**, *61*, e02243–16.
- [31] M. J. Giddins, N. Macesic, M. K. Annavajhala, S. Stump, S. Khan, T. H. McConville, M. Mehta, A. Gomez-Simmonds, A.-C. Uhlemann, *Antimicrob. Agents Chemother.* **2018**, *62*, e02101–17.
- [32] M. A. Taracila, C. R. Bethel, A. M. Hujer, K. M. Papp-Wallace, M. D. Barnes, J. D. Rutter, J. VanPelt, B. A. Shurina, F. Van Den Akker, C. J. Clancy, M. H. Nguyen, S. Cheng, R. K. Shields, R. C. Page, R. A. Bonomo, *Antimicrob. Agents Chemother.* **2022**, *66*, e02124–21.
- [33] G. Haidar, C. J. Clancy, R. K. Shields, B. Hao, S. Cheng, M. H. Nguyen, *Antimicrob. Agents Chemother.* **2017**, *61*, e02534–16.
- [34] P. Gaibani, C. Campoli, R. E. Lewis, S. L. Volpe, E. Scaltriti, M. Giannella, S. Pongolini, A. Berlingeri, F. Cristini, M. Bartoletti, S. Tedeschi, S. Ambretti, *J. Antimicrob. Chemother.* **2018**, *73*, 1525–1529.

- [35] Q. Shi, D. Yin, R. Han, Y. Guo, Y. Zheng, S. Wu, Y. Yang, S. Li, R. Zhang, F. Hu, *Clin. Infect. Dis.* **2020**, *71*, S436–S439.
- [36] C. Venditti, O. Butera, M. Meledandri, M. P. Balice, G. C. Cocciolillo, C. Fontana, S. D'Arezzo, C. De Giuli, M. Antonini, A. Capone, F. Messina, C. Nisii, A. Di Caro, *Clin. Microbiol. Infect.* **2021**, *27*, 1040.e1–1040.e6.
- [37] Q. Liao, J. Deng, Y. Feng, W. Zhang, S. Wu, Y. Liu, H. Che, Y. Xie, *Journal of Infection and Public Health* **2022**, *15*, 545–549.
- [38] E. Antinori, I. Unali, A. Bertoncelli, A. Mazzariol, *Clin. Microbiol. Infect.* **2020**, *26*, 946.e1–946.e3.
- [39] A. Laio, F. L. Gervasio, *Rep. Prog. Phys.* **2008**, *71*, 126601.
- [40] J. M. Sampson, W. Ke, C. R. Bethel, S. R. R. Pagadala, M. D. Nottingham, R. A. Bonomo, J. D. Buynak, F. Van Den Akker, *Antimicrob. Agents Chemother.* **2011**, *55*, 2303–2309.
- [41] G. Bussi, A. Laio, *Nat. Rev. Phys.* **2020**, *2*, 200–212.
- [42] G. Bussi, F. L. Gervasio, A. Laio, M. Parrinello, *J. Am. Chem. Soc.* **2006**, *128*, 13435–13441.
- [43] Y. Naritomi, S. Fuchigami, *J. Chem. Phys.* **2013**, *139*, 215102.
- [44] A. Skliros, M. T. Zimmermann, D. Chakraborty, S. Saraswathi, A. R. Katebi, S. P. Leelananda, A. Kloczkowski, R. L. Jernigan, *Phys. Biol.* **2012**, *9*, 014001.
- [45] N. P. Krishnan, N. O. Nguyen, K. M. Papp-Wallace, R. A. Bonomo, F. Van Den Akker, *PLoS One* **2015**, *10*, e0136813.
- [46] S. C. Mehta, I. M. Furey, O. A. Pemberton, D. M. Boragine, Y. Chen, T. Palzkill, *J. Biol. Chem.* **2021**, *296*, 100155.
- [47] N. K. Stewart, C. A. Smith, H. Frase, D. J. Black, S. B. Vakulenko, *Biochemistry* **2015**, *54*, 588–597.
- [48] R. K. Shields, M. H. Nguyen, E. G. Press, L. Chen, B. N. Kreiswirth, C. J. Clancy, *Antimicrob. Agents Chemother.* **2017**, *61*, e00079–17.
- [49] A. B. Shapiro, S. H. Moussa, N. M. Carter, N. Gao, A. A. Miller, *ACS Infect. Dis.* **2021**, *7*, 79–87.
- [50] A. Bulychev, I. Massova, K. Miyashita, S. Mobashery, *J. Am. Chem. Soc.* **1997**, *119*, 7619–7625.
- [51] C. Huang, B. Zheng, W. Yu, T. Niu, T. Xiao, J. Zhang, Y. Xiao, *IDR* **2018**, *11*, 103–112.
- [52] T. L. Lamoureaux, H. Frase, N. T. Antunes, S. B. Vakulenko, *Antimicrob. Agents Chemother.* **2012**, *56*, 6006–6008.

Manuscript received: November 22, 2023

Accepted manuscript online: January 16, 2024

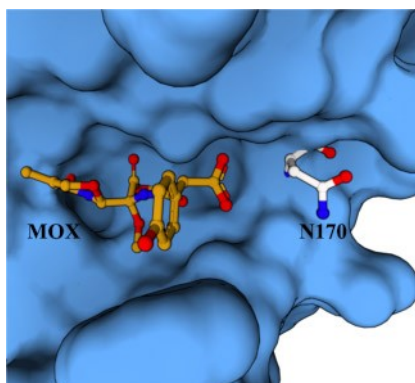
Version of record online: ■■■, ■■■

## Research Articles

## Enzyme Mechanisms

D. Parwana, J. Gu, S. Chen, C. R. Bethel,  
E. Marshall, A. M. Hujer, R. A. Bonomo,  
S. Haider\* \_\_\_\_\_ e202317315

The Structural Role of N170 in Substrate-Assisted Deacylation in KPC-2  $\beta$ -Lactamase



Specific substitutions in the omega loop (R164-D179) of *Klebsiella pneumoniae* carbapenemase 2 (KPC-2) alter its structure and function and can lead to increased resistance to antibiotics. Accelerated rare-event sampling well-tempered metadynamics simulations have now revealed that in D179 variants of KPC-2  $\beta$ -lactamase, the N170 side chain can rotate away from the active site, allowing the binding of antibiotics such as moxalactam and ceftazidime.